

University of Bern, Laboratory for High Energy Physics preprint BUHE-9903

To be published in the New Journal of Physics.

## Charged pion production in fixed target Pb+Pb collisions at 158 GeV per nucleon

### The NA52 collaboration:

G. Ambrosini<sup>a</sup>, R. Arsenescu<sup>a</sup>, C. Baglin<sup>c</sup>, J. Beringer<sup>a</sup>, C. Bohm<sup>e</sup>,  
K. Borer<sup>a</sup>, A. Bussière<sup>c</sup>, F. Dittus<sup>b</sup>, K. Elsener<sup>b</sup>, Ph. Gorodetzky<sup>f</sup>,  
J. P. Guillaud<sup>c</sup>, P. Hess<sup>a</sup>, S. Kabana<sup>a</sup>, R. Klingenberg<sup>a</sup>, T. Lindén<sup>d</sup>,  
K. D. Lohmann<sup>b</sup>, R. Mommsen<sup>a</sup>, U. Moser<sup>a</sup>, K. Pretzl<sup>a</sup>, J. Schacher<sup>a</sup>,  
B. Selldén<sup>e</sup>, F. Stoffel<sup>a</sup>, J. Tuominiemi<sup>d</sup>, M. Weber<sup>a</sup>, Q. P. Zhang<sup>e</sup>

<sup>a</sup> Laboratory for High Energy Physics, University of Bern, Sidlerstrasse 5,  
CH-3012 Bern, Switzerland,

<sup>b</sup> CERN, CH-1211 Geneva 23, Switzerland,

<sup>c</sup> CNRS-IN2P3, LAPP Annecy, F-74941 Annecy-le-Vieux, France,

<sup>d</sup> Dept. of Physics and Helsinki Institute of Physics, University of Helsinki, PO  
Box 9, FIN-00014 Helsinki, Finland,

<sup>e</sup> Dept. of Physics, University of Stockholm, PO Box 6730, S-11385 Stockholm,  
Sweden,

<sup>f</sup> PCC-College de France, 11 place Marcelin Berthelot, 75005 Paris, France

### Abstract.

Changes in pion production as a function of the impact parameter of the collision or the incident energy, may reveal characteristics of a possible first order phase transition from nuclear to quark matter, as predicted by lattice quantum chromodynamics. In this paper we investigate charged pion production in Pb+Pb collisions at 158 GeV per nucleon near zero degree production angle and at forward rapidity ( $4.3 \leq y \leq 6.3$ ). The centrality dependence of pion production is shown in the impact parameter range  $\sim 2$  to 12 fm at the rapidities  $y=5.7$  and 6.3. An enhancement in the  $\pi^-/\pi^+$  ratio has been measured near beam rapidity, indicating Coulomb interaction of charged pions with the spectator protons. The charged pion yield per nucleon participating in the collision ( $N_p$ ) at  $y=5.7$  increases faster than linearly with  $N_p$ , up to  $N_p \sim 100$  and then it saturates, while at  $y=6.3$  it does not exhibit any sudden change as a function of  $N_p$ .

OPEN-99-313  
28/10/99



## 1. Introduction

Pions are the most abundantly produced particles in heavy ion collisions at 158 GeV per nucleon. They carry a large part of the entropy, the other part being carried mostly by baryons. Typically, the number of pions in a central Pb+Pb collision is six times the number of baryons [1]. It is expected that a possible first order phase transition of nuclear matter to quark and gluon matter (the so called Quark Gluon Plasma state –QGP), predicted by quantum chromodynamics on the lattice [2], would result in an enhanced entropy which may show up in a sudden increase of the number of pions as a function of incident energy or impact parameter.

We report in this paper results on invariant differential cross sections and yields of charged pions measured near zero degree production angle in the forward rapidity region ( $4.3 \leq y \leq 6.3$ ) in minimum bias Pb+Pb collisions at 158 GeV per nucleon [3]. Yields are measured as a function of the impact parameter of the collision at  $y=5.7$  and 6.3. Preliminary results of this study were published in [4, 5, 6].

## 2. Experimental setup

The NA52 apparatus uses the H6 beamline of the SPS North Area at CERN as a mass spectrometer. H6 is a 540 m long double-bend focussing beamline which transports charged particles within a momentum acceptance ( $\Delta p/p$ ) of 2.8% and an angular acceptance ( $\Delta\Omega$ ) of  $2.2 \mu\text{sr}$ . The rigidity ( $p/Z$ ) of the spectrometer can be selected between 5 and 200 GeV. Due to the small detector acceptance mostly single particles are detected in the beam line per recorded event.

A schematic diagram of the spectrometer is given in figure 1. The incident lead flux was measured with a 0.4 mm thick segmented quartz Čerenkov counter (TOF0). The target was located in the target ladder noted as target1 in figure 1. During the 1995 run two lead/quartz fiber electromagnetic calorimeters (QFC) [7, 8] of 25 radiation lengths ( $X_0$ ) with pseudorapidity acceptance of  $2.7 < \eta < 4.1$ , positioned 0.6 m downstream of the target were used to measure the impact parameter of the collision. A set of scintillation counters, 8-fold segmented time-of-flight hodoscopes (TOF1-5) and three beam counters (B0-2) allowed to determine the charge and the velocity of the particles transported in the beam line. Three threshold (Č0, Č1, Č2) and one differential (CEDAR) Čerenkov counters provided additional particle identification capabilities. Seven multiwire proportional chambers (W1T-W5T, W2S, W3S) were used for tracking measurements.

A segmented uranium/scintillator hadronic calorimeter was installed at the end of the beam line to provide pion identification. The calorimeter [9] has a total depth of 7.1 interaction lengths and is longitudinally segmented in five modules (figure 2), each made from uranium absorber plates alternating with scintillator plates. The trigger and data acquisition systems were implemented in two independent parts, allowing for recording events either over the full length of the spectrometer for the study of particles with a life time of at least  $1.8 \mu\text{s}$ , or only up to the counter B1 for particles with a life time of at least  $0.9 \mu\text{s}$ . A more detailed description of the experimental setup can be found in Ref. [9].

### 3. Experimental method

The  $(m/Z)^2$  spectrum in figure 3 illustrates the particle identification capability of the time-of-flight measurements. As is seen from the figure, electrons, muons and pions can not be separated with this method. The calorimeter information provides a way to identify these light particles. Figure 4 demonstrates the method of particle separation with the hadronic calorimeter at a spectrometer rigidity of 20 GeV. Figure 5 shows the result of the combined particle identification using the time of flight and the calorimeter information at 20 GeV rigidity. At lower rigidities ( $p/Z \leq 10$  GeV) particle identification was performed by means of the threshold Čerenkov counters Č0 and Č1.

Data were taken at spectrometer rigidities  $p/Z$  of  $\pm 5$ ,  $\pm 10$ ,  $\pm 20$  and  $\pm 40$  GeV (corresponding to pion rapidity of  $y=4.3$ ,  $5.0$ ,  $5.7$  and  $6.3$ ) with a 4 mm thick lead target. The pion cross sections were measured between 5 to 40 GeV rigidity ( $p/Z$ ) since the lowest tunable rigidity for the H6 beamline is 5 GeV and the separation of pions from other hadrons was not possible for rigidities  $p/Z > 40$  GeV because of the limited resolution of the time-of-flight measurements and of the threshold Čerenkov counters. Empty target runs were taken in order to take into account the contribution of interactions outside the target.

At rapidities 5.7 and 6.3 the invariant pion yields have been investigated as a function of the mean total number of nucleons participating in the collision. In the runs at rapidity  $y=4.3$  and  $5.0$  the lead/quartz fiber calorimeters were not available, therefore no information on the centrality of the collision exists for these data samples.

The particle yields are investigated in five centrality regions. The mean total number of participant nucleons in the collision in each centrality region has been deduced by comparing the energy spectrum of the lead/quartz fiber calorimeter with the energy spectrum obtained within the event generator VENUS 4.12 [10]. The experimental energy resolution was implemented in the generator. The cross section in each centrality region was obtained by integrating the calorimeter energy spectrum over an energy interval:

$$\sigma_{cut} = \int_{E_{min}}^{E_{max}} \frac{d\sigma}{dE} dE \quad (1)$$

The resulting cross section, the mean number of participating nucleons and the mean impact parameter of each centrality region are shown in table 1. For a more detailed description of the centrality dependence analysis see [11].

The particle cross sections and yields have been calculated taking into account the absorption of the incident ions in the target and their pile up in the electronic readout of the quartz counter, the spectrometer acceptance, the particle decay, interactions with material in the beamline, absorption in the target and the reconstruction efficiency. For more details on these corrections see reference [12]. The number of empty target background events was subtracted for each centrality bin. Reinteractions in the target were not corrected.

The systematic error of the cross sections due to uncertainties in the spectrometer

acceptance are estimated to be  $\sim 15\%$ . The systematic error due to uncertainties in the empty target correction is  $\sim 10\%$  ([3], [11]). In the systematic error of the pion invariant yields an additional contribution of  $\sim 7\%$  due to the centrality analysis [11] has to be added. The resulting total systematic error for the pion cross sections is  $\sim 18\%$  and for the pion yields  $\sim 19\%$ , where the different contributions to the systematic error have been quadratically added. The error on the mean number of participating nucleons is  $\sim 13\%$  [11]. In the following only the statistical errors are shown unless stated differently.

#### 4. Results

The transverse momentum ( $p_T$ ) acceptance of the particles ranges from zero to a maximum  $p_T$  value, which is different for each rigidity and can be calculated as:  $p_T(max) \sim 0.0013 \cdot p$ , with  $p$  being the momentum of the particle (see reference [13] for a discussion of the spectrometer acceptance). The invariant differential pion cross sections in minimum bias Pb+Pb collisions at 158 GeV per nucleon are shown in table 2 and in figures 6 and 7 as a function of rapidity. The results on  $K^+$ ,  $p$ ,  $d$ ,  ${}^3\text{He}$ ,  $t$ ,  $K^-$ ,  $\bar{p}$ ,  $\bar{d}$  and  $\overline{{}^3\text{He}}$  production in figure 6 and 7 were published in Ref. [12]. Figure 8 shows the resulting antiparticle to particle ratios as a function of rapidity. The  $\pi^-/\pi^+$  ratio is found to peak around  $y=5.7$ .

The invariant pion yields are shown in table 3 for rapidities 5.7 and 6.3 and for different centrality regions. Figures 9 and 10 show the invariant yield of  $\pi^+$  and  $\pi^-$  at  $y=5.7$  and 6.3 divided by the mean number of participants  $N_p$  as a function of  $N_p$ . The p+Be data [14] shown in the same pictures have been measured near zero  $p_T$  and at the same ratio of rapidity over beam rapidity ( $y/y_{beam}$ ) as the Pb+Pb data. They were measured at an incident beam energy of 450 GeV per nucleon and have been rescaled to the incident energy of 158 GeV per nucleon. The systematic error on the particle yields in p+Be interactions is between 5 and 10% depending on the beam momentum [14]. The systematic error in the NA56 experiment is improved as compared to the NA52 measurements though they use the same apparatus, because they were performed with different beam line conditions improving the acceptance uncertainties in the NA56 experiment. The energy rescaling factors were calculated from the measured energy dependence of the total  $\pi^\pm$  multiplicities in p+p collisions [15]. The mean number of participants in p+Be collisions was estimated with VENUS 4.12 to be  $N_p=2.34 \pm 0.06$ . The total cross section for the reaction p+Be was taken from [16] to be  $\sigma=0.268$  barn (for energy between 80 and 240 GeV). Figure 11 show the  $\pi^-/\pi^+$  ratios at rapidities 5.7 and 6.3 as a function of the mean number of participant nucleons.

#### 5. Discussion

The enhancement in the  $\pi^-/\pi^+$  ratio near beam rapidity (figure 8) may be interpreted as being due to Coulomb interaction between the charged pions and the spectator protons. This effect would result in more  $\pi^-$  than  $\pi^+$  falling into the small forward angular acceptance of the spectrometer. The enhancement is larger than would be expected from the excess of neutrons over protons in the lead nuclei, which yields a  $\pi^-/\pi^+$  ratio of about 1.1. Another possible source of an enhanced  $\pi^-$  to  $\pi^+$  ratio is

the associated production of  $\Lambda\bar{K}$ . According to a simulation based on VENUS this contribution as well as the initial isospin asymmetry yields a  $\pi^-/\pi^+$  ratio of 1.2, which cannot explain the observed effect.

An enhancement of the  $\pi^-/\pi^+$  ratio was also observed in Pb+Pb collisions by the NA44 experiment [17], however at midrapidity and for central collisions. This has also been interpreted as being due to Coulomb interactions.

The  $\pi^+$  invariant yield divided by the number of participants  $N_p$  increases, whereas the  $\pi^-$  yield over  $N_p$  decreases with  $N_p$  for both investigated rapidities (figures 9, 10). In these figures also p+Be data are displayed where measurements were available. Based on the expectation that both the positive and negative pion yields in peripheral Pb+Pb events should be equal or larger than in p+Be collisions at the same energy, the behaviour seen in figure 9 is indicative of Coulomb interaction enhancing the  $\pi^-$  and decreasing the  $\pi^+$  yields in the most peripheral Pb+Pb data. Furthermore in p+Be reactions near beam rapidity and zero  $p_T$  the presence of only one incident proton in the beam implies a higher  $\pi^+$  than  $\pi^-$  yield, due to isospin and charge conservation. Indeed the  $\pi^-/\pi^+$  ratio in p+Be at  $y/y_{beam} = 0.98$  drops to  $\sim 0.55$  (see figure 12). Both effects are suppressed when going away from beam rapidity. This is in line with figure 10, which shows that at rapidity 1.1 the  $\pi^+$  yields in peripheral Pb+Pb are higher than in p+Be collisions.

The  $\pi^-/\pi^+$  ratio at  $y=5.7$  and  $6.3$  decreases with increasing centrality of the collision (figure 11). The decrease is stronger for  $y=5.7$ . The  $\pi^-/\pi^+$  ratio is larger than one reaching a maximum value of  $\sim 7$  in the most peripheral events at  $y=5.7$ . This rapidity and centrality dependence of the  $\pi^-/\pi^+$  ratio further supports the hypothesis of Coulomb interactions of charged pions with the projectile spectators. The Coulomb interaction near beam rapidity and zero  $p_T$  is expected to be strongest for the most peripheral events, for which the number of spectator protons is largest. It is expected to be smallest when looking at central events in this phase space region since with increasing number of nucleons participating in the collision the positive charge is shifted towards midrapidity and higher  $p_T$  values. Furthermore the  $\pi^-/\pi^+$  ratio is expected to be smaller at  $y=6.4$  than at  $y=5.7$  because of the fact that the latter is nearer to the beam rapidity where the Coulomb effect is more pronounced.

Figure 12 shows the  $\pi^-/\pi^+$  ratio as a function of the rapidity normalized to the beam rapidity ( $y/y_{beam}$ ), for the most central, the most peripheral and the minimum bias Pb+Pb events as well as for central Au+Au collisions at 10.8 GeV per nucleon [18] and p+Be collisions at 450 GeV per nucleon [14]. A similar increase of the  $\pi^-/\pi^+$  ratio near beam rapidity due to the Coulomb interaction is expected in Pb+Pb and Au+Au collisions at the same centrality, independent of the incident energy per nucleon, since the number of spectators is about the same. On the contrary, the  $\pi^-/\pi^+$  ratio measured in p+Be interactions at 450 GeV per nucleon near zero  $p_T$  do not exhibit any enhancement near  $y_{beam}$ , instead it remains below one.

In order to search for dependence of the pion production properties on the number of participants that could reveal a possible phase transition we have studied the geometrical mean of the invariant  $\pi^+$  and  $\pi^-$  yields ( $\sqrt{\pi^+ \cdot \pi^-}$ ) divided by the number of participants  $N_p$  as a function of  $N_p$ . The leading Coulomb correction in an

environment of positive charge behaves as  $e^{-X}$  (repulsive) for  $\pi^+$ , with  $X$  being a positive function of the fine structure constant  $\alpha$  and the momentum  $k$ . Similarly for  $\pi^-$  the correction is  $e^{+X}$  (attractive). The geometrical mean of the yields eliminates this correction to a large extent, whereas for the arithmetic mean it is not corrected. On the other hand for the geometrical mean the isospin asymmetries are not corrected, while this is the case for the arithmetic mean. We assume therefore that the influence of Coulomb interaction at this particular rapidity and  $p_T$  is larger than the influence of the asymmetry between proton and neutron numbers. This assumption is supported by the comparison of the data to the VENUS event generator and by our calculation of the  $\pi^-/\pi^+$  ratio due to isospin asymmetry in the lead nucleus as discussed previously. This quantity is plotted in figure 13 together with p+Be data at 158 GeV per nucleon. The Coulomb corrected pion yield per participant nucleon in Pb+Pb collisions at  $y=5.7$  increases with centrality up to  $N_p = 100$  and then it saturates. The straight line extrapolation of the spectrum towards small  $N_p$  points back to the p+Be value. In central Pb+Pb events the pion yield per  $N_p$  is larger than in p+Be collisions. The  $N_p$  dependence of the pion yield per participating nucleon seen in the Pb+Pb data at  $y=5.7$  can be interpreted as non thermal pion production for  $N_p < 100$  and a higher degree of equilibration for  $N_p > 100$ .

The pion invariant cross sections are compared to those of charged kaons [12] at the same rapidity and  $p_T$  in table 4. The  $K/\pi$  ratio measures any excess production of  $s\bar{s}$  quarks compared to the production of  $u\bar{u}$  or  $d\bar{d}$  quarks. The interest for this observable arises from the theoretical expectation of an enhanced  $s\bar{s}$  quark as compared to light ( $u, d$ ) quark production in case of a QGP phase transition [19]. The  $K^+/\pi^+$  ratio in minimum bias Pb+Pb data at  $y=4.3$  is  $\sim 1.5 \pm 0.4$  times the one in p+Be data, whereas the  $K^-/\pi^-$  ratio at  $y=4.3$  and the  $K^+/\pi^+$  ratio at  $y=5.0$  are the same. The observation of a modest enhancement of the kaon to pion ratio at forward rapidity in minimum bias Pb+Pb collisions, is not in contradiction with the possibility of a QGP formation since the measurement is in forward rapidity and near zero  $p_T$ . In particular since the kaon to pion ratio is expected to be maximal at midrapidity due to the maximal available energy and at higher  $p_T$  due to the presence of transverse flow [25]. Indeed an enhancement of a factor of  $\sim 2$  in strange particle to pion ratios in Pb+Pb and other heavy ion collisions, as compared to p+A collisions at the same energy, was observed around midrapidity [20, 21].

Assuming that local thermal equilibrium is reached for the pions at all centralities we can estimate the centrality dependence of the entropy per baryon. This assumption is not supported for events with less than 100 participants as it is inferred from figure 13 but some degree of local equilibration among pions in peripheral events is not excluded. Figure 14 shows the centrality dependence of the entropy per baryon calculated within a thermal model as [22]:

$$S/B = 3.95 - \ln(d/p) + 4.1(\pi/p) \quad (2)$$

The deuterons and protons have been measured at  $y=3.7$ , the protons at  $y=4.4$  [11] and the pions ( $\sqrt{\pi^+\pi^-}$ ) at  $y=5.7$ . The entropy per baryon in the mostly forward rapidity hemisphere ( $3.7 \leq y \leq 5.7$ ) is seen to increase with centrality. Since the entropy per baryon should not depend on the volume, this increase cannot be understood as due to the enlarged freeze-out volume of the system [11]. It could be a consequence of the increased energy density in the more central events. The centrality

bins used in the figures 13 and 14 are subdivisions of the centrality regions presented in table 1 (see [11] for more informations). Note that due to the presence of collective transverse flow [25] the ratios of particles with different masses near zero transverse momentum and all parameters estimated from them like S/B differ from their values measured over the full  $p_T$  range. Furthermore the centrality dependence of the  $\pi/p$  ratio, measured within our small rapidity range, is sensitive to changes of the baryon rapidity distribution with centrality.

## 6. Conclusions

We present results on  $\pi^+$  and  $\pi^-$  invariant production cross sections in minimum bias Pb+Pb interactions at 158 GeV per nucleon in the rapidity range  $4.3 \leq y \leq 6.3$  and near zero degree production angle. The centrality dependence of the charged pion yields were investigated at  $y=5.7$  and  $6.3$ .

The ratio of the  $\pi^-$  over  $\pi^+$  yields show a significant maximum near beam rapidity, 7 for the peripheral events, 1.8 for the central events. The effect may be due to Coulomb interactions between the pions and the spectator protons. It cannot be explained by other sources like the initial isospin asymmetry of the Pb nucleus or by associated  $\Lambda\bar{K}$  production, which yield a  $\pi^-/\pi^+$  ratio of 1.2 only.

The Coulomb corrected charged pion yield ( $\sqrt{\pi^+\pi^-}$ ) measured at  $y=5.7$  per participating nucleon increases with centrality up to  $N_p = 100$  and then it saturates. The straight line extrapolation of the spectrum towards small  $N_p$  points back to the p+Be value. The charged pion yield per participant nucleon is larger in central Pb+Pb than in p+Be collisions. Pion yields at  $y=6.3$  increase slightly less than linearly with  $N_p$  and show no sudden change as a function of  $N_p$ .

The  $K^+/\pi^+$  ratio at  $y=4.3$  is slightly larger than in p+Be collisions at the same energy, whereas the  $K^+/\pi^+$  ratio at  $y=5.0$  as well as the  $K^-/\pi^-$  ratio at  $y=4.3$  are the same for both data. These observations do not contradict the measured increase by a factor of  $\sim 2$  of the  $p_T$  integrated strange particle to pion ratios in heavy ion reactions compared to p+A collisions at the same energy, since the latter occurs mostly around midrapidity.

The entropy per baryon extracted from the  $\pi/p$  and  $d/p$  ratios at forward rapidity and near zero transverse momentum assuming thermal equilibrium is seen to increase with increasing collision centrality.

## Acknowledgments

We thank Prof. U. Heinz and Prof. P. Minkowski for fruitful discussions.

## References

- [1] H. Appelshäuser et al. (NA49 Coll.), nucl-ex/9810014.
- [2] E. Laermann, Quark Matter '96 Proc., Nucl. Phys. A610 (1996) 1c.
- [3] Renius Arsenescu Ph. D. Thesis, University of Bern, 1999.

- [4] R. Arsenescu et al. (NA52 Coll.), Journal of Physics G, Nuclear and Particle Physics, Vol. 25 (1999) 225.
- [5] S. Kabana et al. (NA52 Coll.), Journal of Physics G, Nuclear and Particle Physics, Vol. 25 (1999) 217.
- [6] S. Kabana et al.(NA52 coll.), contribution to the International Conference on Quark Matter, 10-15 May 1999, Torino, Italy, to be published in the proceedings.
- [7] M. Weber et al (NA52 Coll.), Proceedings of the VII International Conference on Calorimetry in High Energy Physics, 9-14 Nov. 1997, Tucson, Arizona, USA, Proceedengs edited by E. Cheu et al., World Scientific Publishing Co. Pte. Ltd. (1998) 151, Univ. of Bern preprint BUHE-97-10.
- [8] M. Weber, Diploma Thesis, University of Bern, 1996, <http://www.lhep.unibe.ch/newmass/publications/theses/theses.html>.
- [9] Pretzl K. et al. (NA52 Coll.), Proc. Conf. of International Symposium on Strangeness and Quark Matter 1994, Krete, Greece, World Scientific (1995) 230.
- [10] K. Werner, Phys.Rep. 232 (1993) 87.
- [11] Impact parameter dependence of  $K^\pm$ ,  $p$ ,  $\bar{p}$ ,  $d$  and  $\bar{d}$  production in Pb+Pb collisions at 158 GeV per nucleon, G. Ambrosini et al. (NA52 Coll.), submitted to New Journal of Physics.
- [12] Ambrosini G et al. (NA52 Coll.) Phys. Lett. B 417 (1998) 202.
- [13] R. Klingenberg, Ph. D. Thesis, University of Bern, March 1996, <http://www.lhep.unibe.ch/newmass/publications/theses/theses.html>.
- [14] G. Ambrosini et al. (NA56 Coll.), submitted to European Journal of Phys. C. G. Ambrosini et al. (NA56 Coll.), Phys. Lett. B 420 (1998) 225.
- [15] E. Albin et al., Nucl. Phys. B 84 (1975) p. 269.
- [16] Review of Particle Properties, Physical Review D Particles and Fields Vol. 50 (1994) p. 1241.
- [17] H. Boggild et al. (NA44 Coll.) Phys. Lett. B 372 (1996) 339.
- [18] R. Lacasse et al. (E877 Coll.), Nucl. Phys. A 610(1996) p. 153c.
- [19] P. Koch, B. Müller and J. Rafelski, Phys. Rep. 142 (1986) 167.
- [20] T. Alber et al., (NA35 Coll.), Z. Phys. C 64 (1994) p. 195.
- [21] P.Seyboth, Journal of Physics G: Nuclear and Particle Physics, Vol. 23 Number 12 (1997), p. 1787.
- [22] J. Barrette et al., Phys. Rev. C 50, 2, (1994) 1077.
- [23] F. Stoffel, Ph. D. Thesis, University of Bern 1997, <http://www.lhep.unibe.ch/newmass/publications/theses/theses.html>.
- [24] E. Andersen et al., (NA36 coll.) Phys. Lett. B 220 (1989) 328.
- [25] International Conference on ultrarelativistic nucleus nucleus collisions, Quark matter '99, 10-15 May 1999, Torino, Italy for example see contribution of U. Heinz in the Proceedings.



centrality cut	$\sigma_{cut}$ (barn)	$\langle N_p \rangle$	$\langle b \rangle$ (fm)
no cut	$8.2 \pm 2.0$	$103 \pm 2$	$10.25 \pm 0.09$
1	$2.483 \pm 0.034$	$62.5 \pm 0.5$ (41.7)	$11.00 \pm 0.02$ (1.7)
2	$1.379 \pm 0.019$	$149.3 \pm 0.9$ (58.7)	$8.15 \pm 0.02$ (1.6)
3	$0.835 \pm 0.013$	$236.8 \pm 1.2$ (63.6)	$5.81 \pm 0.03$ (1.7)
4	$0.505 \pm 0.010$	$297.8 \pm 1.3$ (55.5)	$4.13 \pm 0.04$ (1.6)
5	$0.253 \pm 0.001$	$336.3 \pm 1.6$ (42.6)	$3.02 \pm 0.05$ (1.4)

**Table 1.** Cross section ( $\sigma_{cut}$ ), mean number of participant nucleons in the collision ( $\langle N_p \rangle$ ) and mean impact parameter ( $\langle b \rangle$ ) for the five centrality bins used in the tables 4 and 5 and in most figures.  $\sigma_{cut}$  is the cross section of each centrality region, defined as  $\sigma_{cut} = \int_{E_{min}}^{E_{max}} \frac{d\sigma}{dE} dE$ . The first line of the table corresponds to minimum bias Pb+Pb collisions (no centrality cut) and the corresponding cross section has been found [23] from a parametrization of experimental data taken from reference [24]. The errors shown are the statistical errors, while the values in parenthesis are the standard deviations of the distributions in the considered centrality ranges.

	$E \frac{d^3\sigma}{dp^3}$ (barn GeV <sup>-2</sup> )	$E \frac{d^3\sigma}{dp^3}$ (barn GeV <sup>-2</sup> )	$E \frac{d^3\sigma}{dp^3}$ (barn GeV <sup>-2</sup> )	$E \frac{d^3\sigma}{dp^3}$ (barn GeV <sup>-2</sup> )
	y=4.3	y=5.0	y=5.7	y=6.3
$\pi^+$	620.4 ± 20.0	474.7 ± 15.0	186.9 ± 5.8	126.4 ± 3.8
$\pi^-$	602.0 ± 21.8	718.1 ± 26.0	565.2 ± 13.9	188.1 ± 2.3

**Table 2.** Invariant cross sections of  $\pi^+$  and  $\pi^-$  produced in minimum bias Pb+Pb collisions at 158 GeV per nucleon and near zero transverse momentum as a function of rapidity.

cuts	$2\pi E \frac{d^3N}{dp^3}$ (GeV <sup>-2</sup> )	$2\pi E \frac{d^3N}{dp^3}$ (GeV <sup>-2</sup> )	$2\pi E \frac{d^3N}{dp^3}$ (GeV <sup>-2</sup> )	$2\pi E \frac{d^3N}{dp^3}$ (GeV <sup>-2</sup> )
	$\pi^+$ y=5.7	$\pi^+$ y=6.3	$\pi^-$ y=5.7	$\pi^-$ y=6.3
1	42.2 ± 3.2	41.3 ± 4.2	293.4 ± 24.4	106.8 ± 16.7
2	162.0 ± 8.8	108.8 ± 8.0	649.2 ± 34.7	249.7 ± 23.8
3	309.2 ± 16.16	178.0 ± 12.6	780.6 ± 40.0	298.0 ± 27.0
4	475.9 ± 25.6	233.8 ± 17.0	900.0 ± 47.5	320.7 ± 29.2
5	562.5 ± 34.5	227.3 ± 18.8	961.1 ± 55.8	299.1 ± 28.1

**Table 3.** Invariant yields of  $\pi^+$  and  $\pi^-$  produced in Pb+Pb collisions at 158 GeV per nucleon and near zero transverse momentum as a function of rapidity and centrality.

$y(\text{Pb}+\text{Pb})$	$y/y_{beam}$	$K^+/\pi^+$	$K^-/\pi^-$
		Pb+Pb	Pb+Pb
4.3	0.74	$0.055 \pm 0.014$	$0.026 \pm 0.007$
5.0	0.86	$0.045 \pm 0.012$	$0.0102 \pm 0.003$
		p+Be 158 GeV/N	p+Be 158 GeV/N
4.3	0.74	$0.036 \pm 0.003$	$0.025 \pm 0.004$
5.0	0.86	$0.032 \pm 0.004$	

**Table 4.** Charged kaon to pion ratios near zero  $p_T$  and at rapidities  $\sim 4.3$  and  $5.0$  in minimum bias Pb+Pb collisions at 158 A GeV and in p+Be collisions at 450 GeV per nucleon [14]. The latter were rescaled to 158 GeV per nucleon. The errors quoted include systematic and statistical errors.

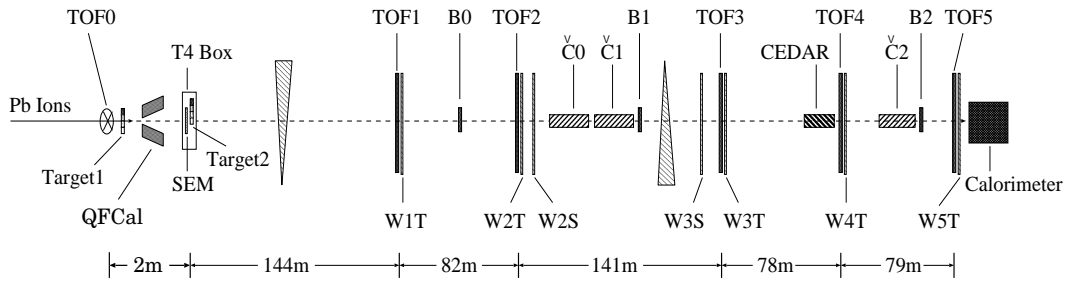


**Figure 1.** The NA52 experimental set up.

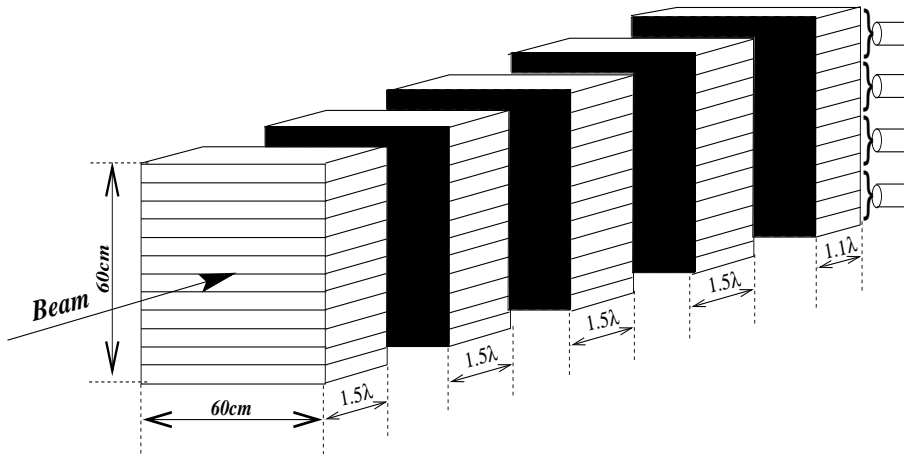


**Figure 2.** The hadronic calorimeter.

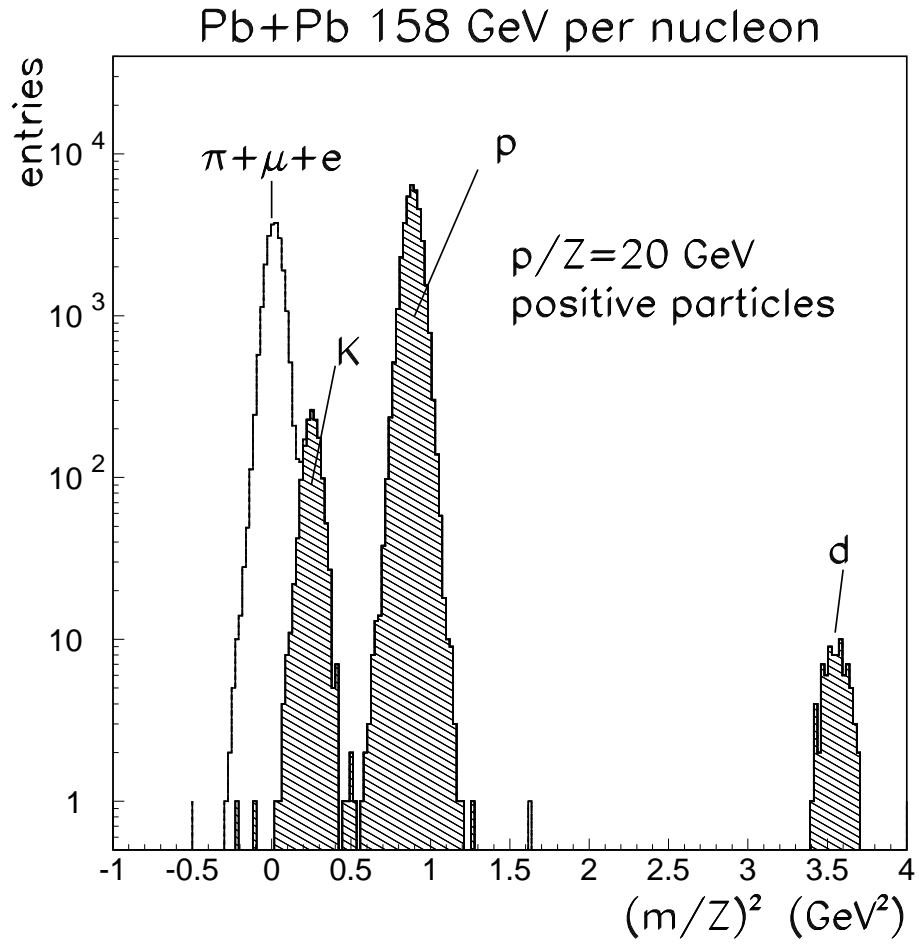


**Figure 3.** Typical example of a  $(m/Z)^2$  spectrum of positive particles obtained from time-of-flight measurements at  $p/Z = 20$  GeV. The shaded area indicates particles which gave no light in the Čerenkov counter.

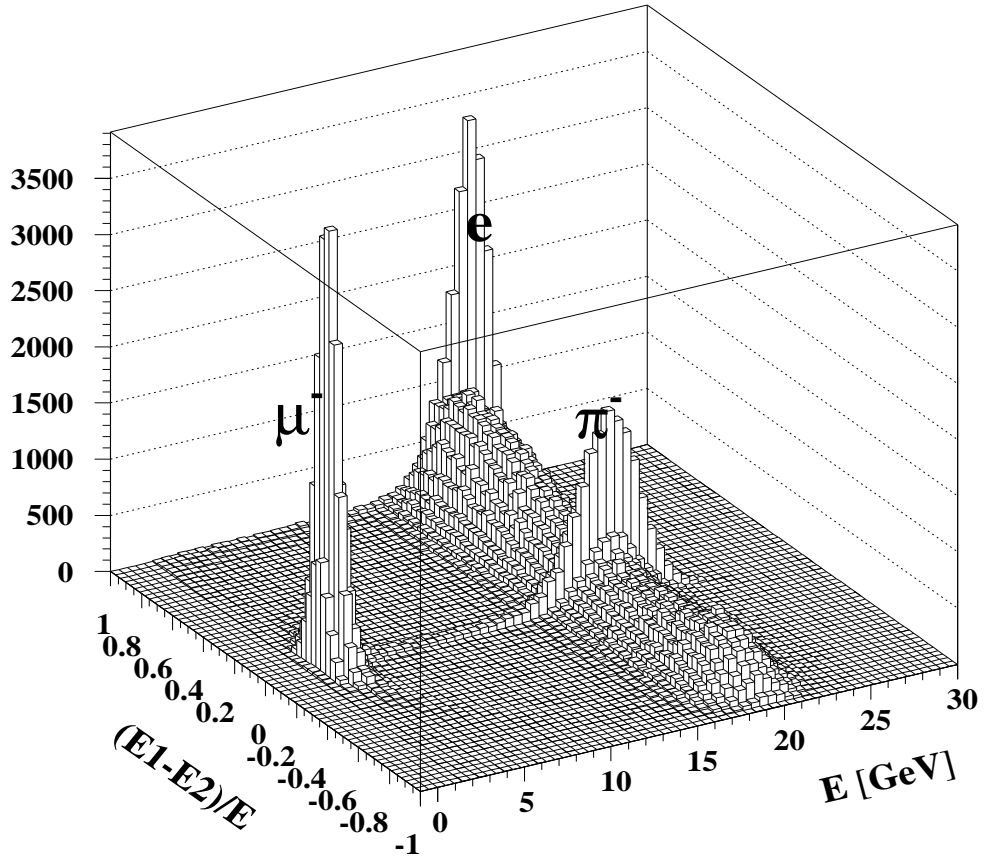


**Figure 4.** Difference of the energy deposited in the first and second hadronic calorimeter module ( $E1 - E2$ ) over the total energy deposited in the calorimeter  $E$ , displayed as a function of the latter, for negative particles with  $p/Z = 20$  GeV.

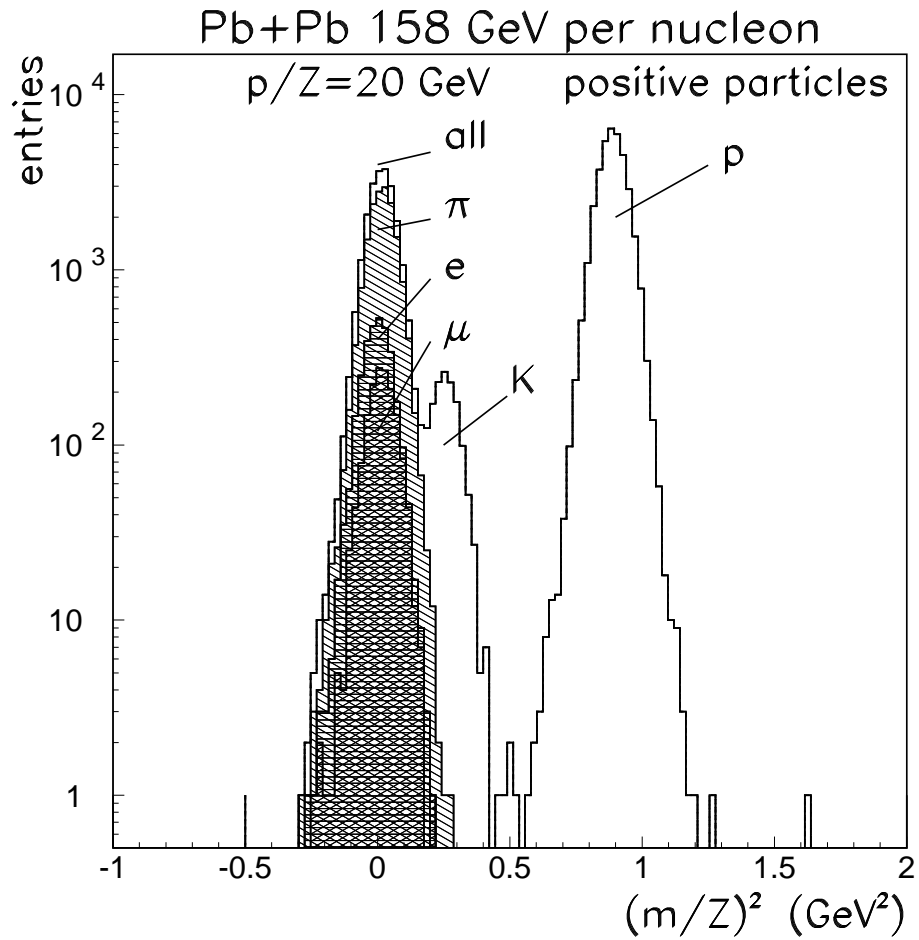


**Figure 5.** Typical example of particle identification at  $p/Z = 20$  GeV/c.  $K^+$ , p and heavier particles are separated using TOF information, while  $\pi^+$ ,  $\mu^+$  and  $e^+$  are identified using calorimeter and Čerenkov information.

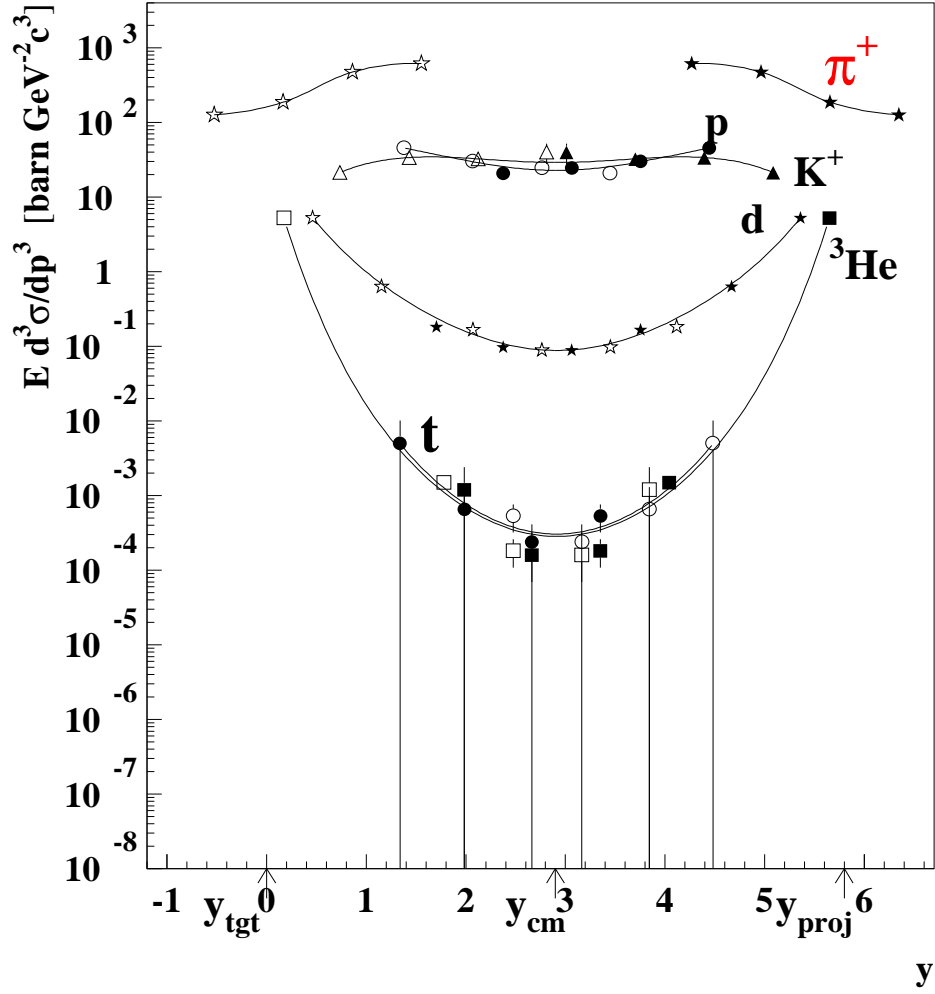


**Figure 6.** Invariant production cross sections of positive particles and nuclei in minimum bias Pb+Pb collisions at 158 A GeV near zero  $p_T$ . Closed symbols refer to the measured points; the open symbols are points reflected over midrapidity ( $y_{cm} = 2.9$ ). The lines are drawn to guide the eye.



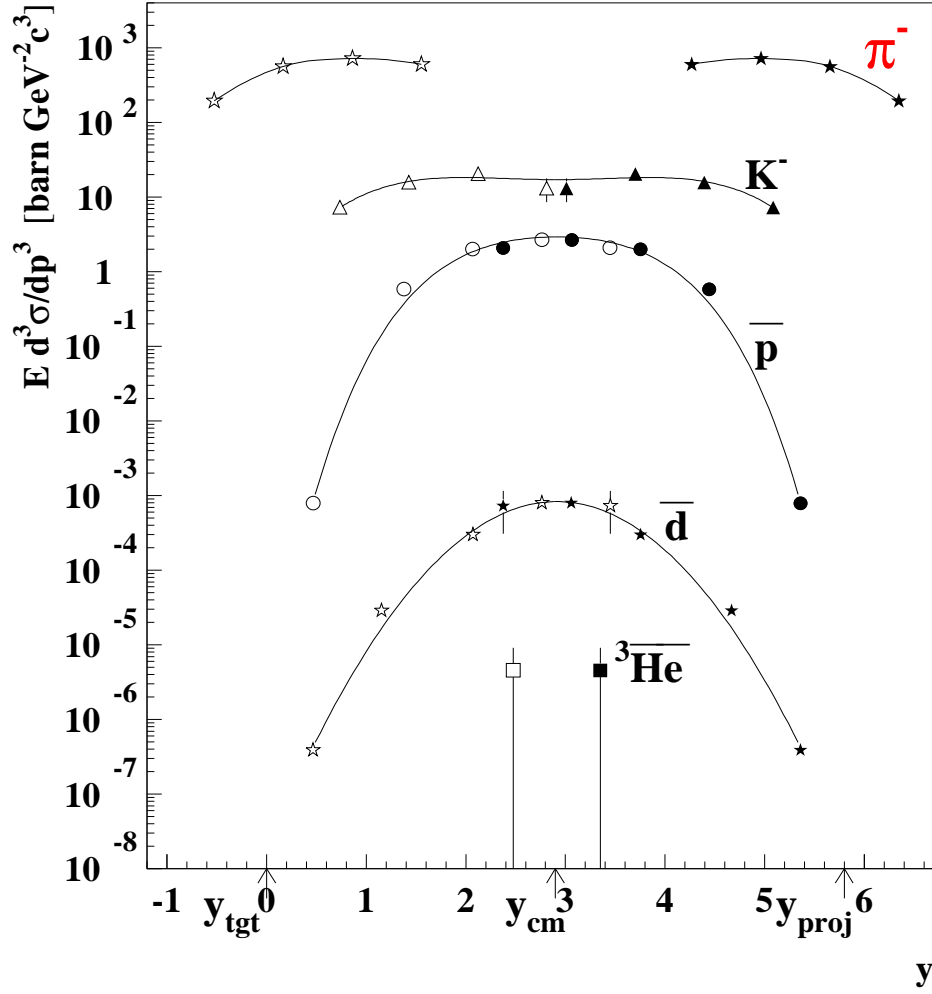


**Figure 7.** Invariant production cross sections of negative particles and antinuclei in minimum bias Pb+Pb collisions at 158 A GeV near zero  $p_T$ . Closed symbols refer to the measured points; the open symbols are points reflected over midrapidity ( $y_{cm} = 2.9$ ). The lines are drawn to guide the eye.

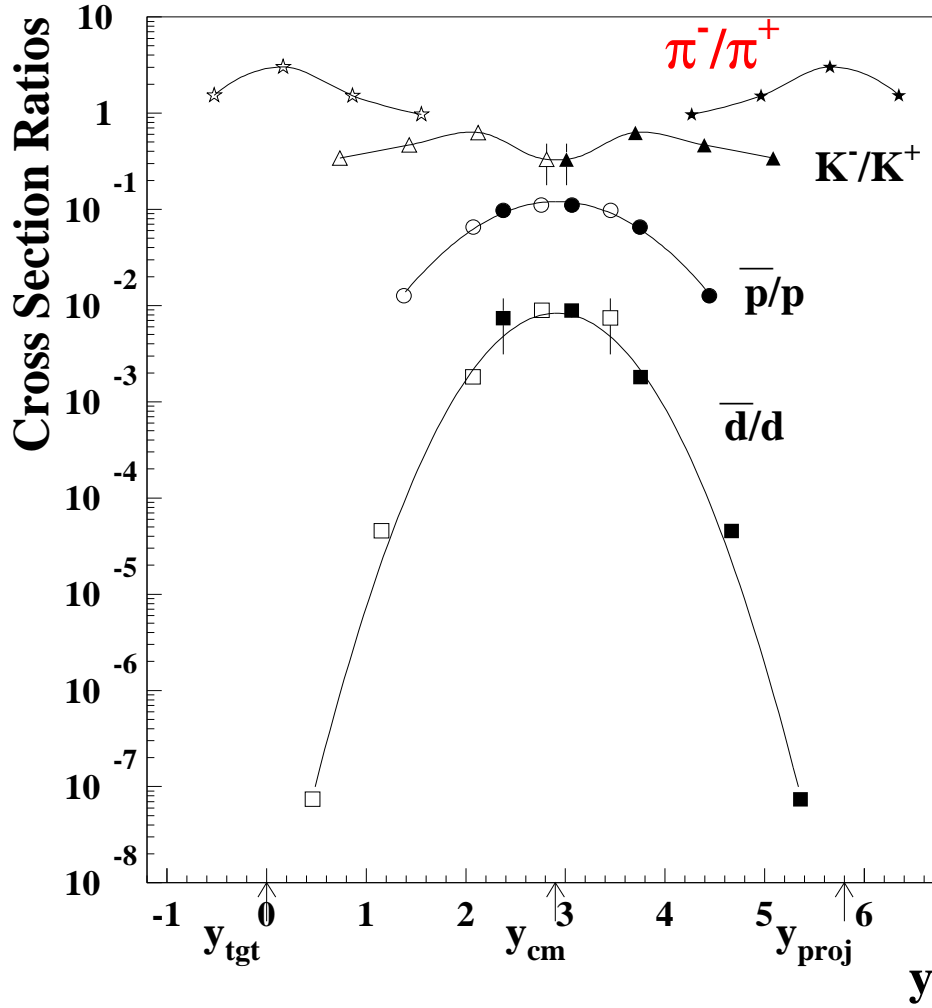


**Figure 8.** Rapidity dependence of particle cross section ratios in minimum bias Pb+Pb collisions at 158 A GeV near zero  $p_T$ . Closed symbols refer to the measured points; the open symbols are points reflected over midrapidity ( $y_{cm} = 2.9$ ). The lines are drawn to guide the eye.

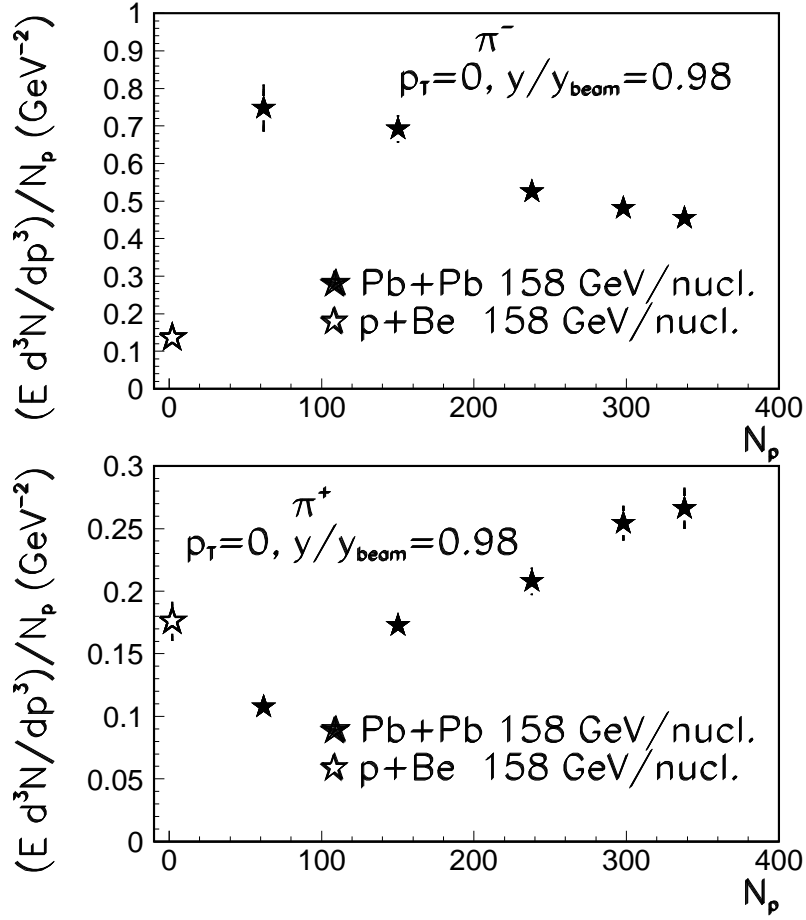


**Figure 9.** Charged pion invariant yields in Pb+Pb collisions at 158 A GeV near zero  $p_T$  divided by the mean number of participating nucleons in the reaction ( $N_p$ ) as a function of  $N_p$  at rapidity 5.7. The p+Be data were measured at 450 GeV per nucleon at the same  $p_T$  and  $y/y_{beam}$  [14] and have been rescaled to 158 A GeV (see text).

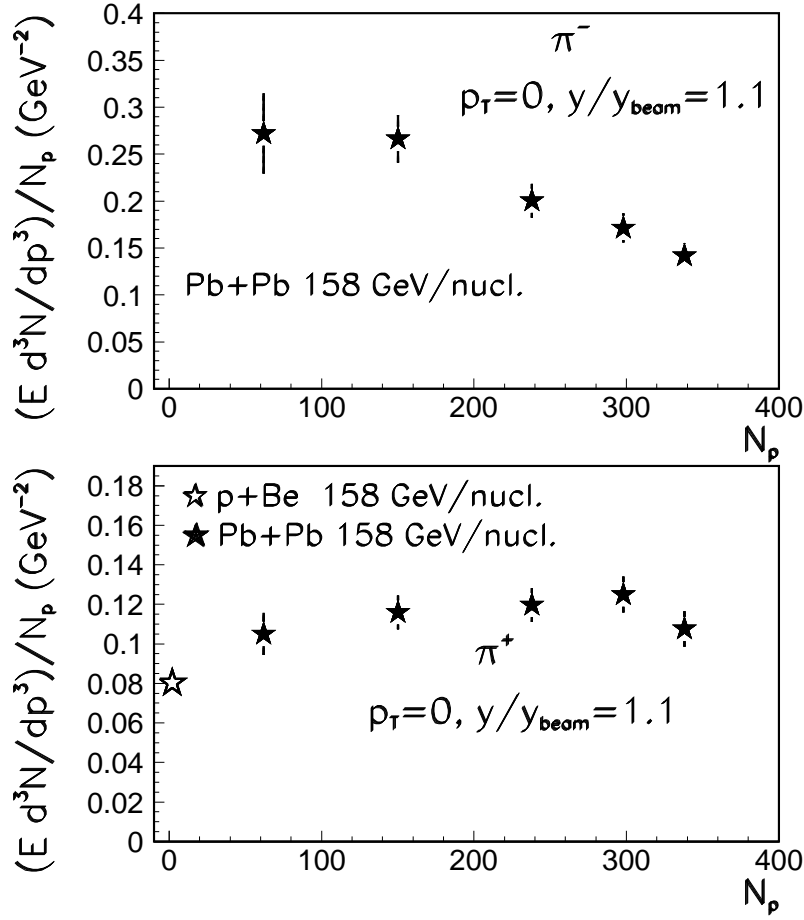


**Figure 10.** Charged pion invariant yields in Pb+Pb collisions at 158 A GeV near zero  $p_T$  divided by the mean number of participating nucleons in the reaction ( $N_p$ ) as a function of  $N_p$  at rapidity 6.3. The p+Be data were measured at 450 GeV per nucleon in the same  $p_T$  and  $y/y_{\text{beam}}$  [14] and have been rescaled to 158 A GeV (see text).

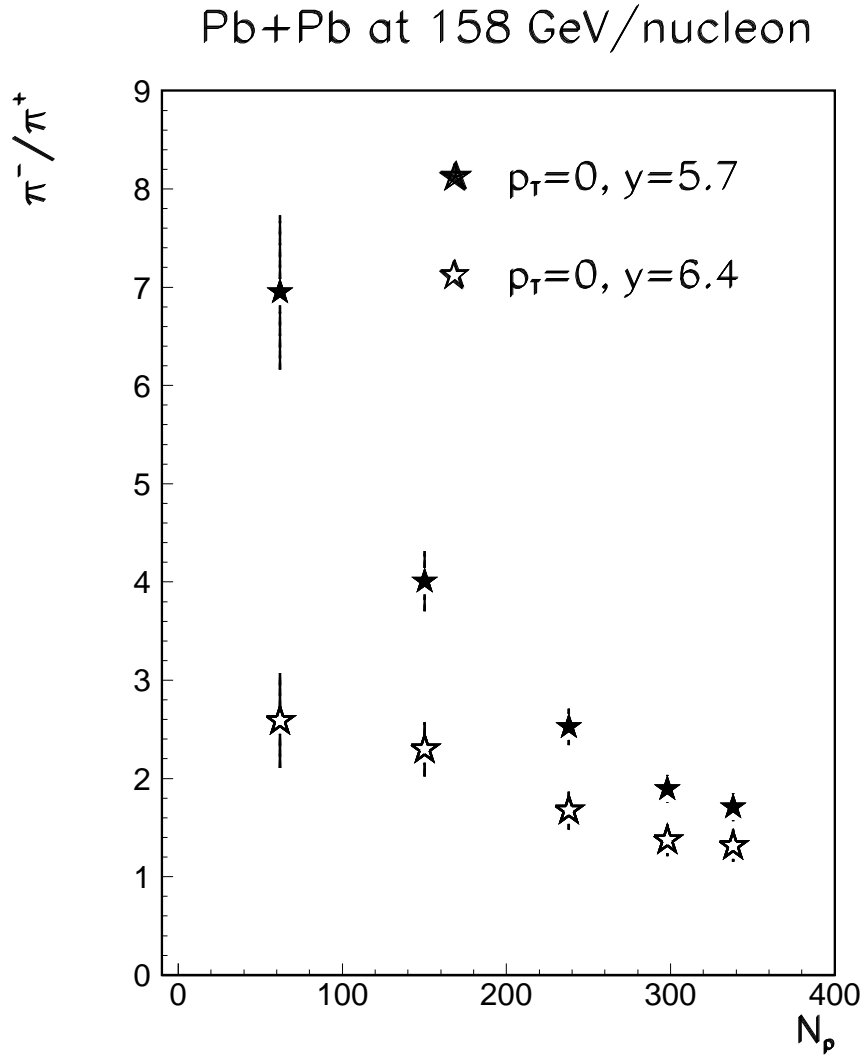


**Figure 11.**  $\pi^-/\pi^+$  ratio in Pb+Pb collisions at 158 GeV per nucleon near zero  $p_T$  as a function of the mean number of participating nucleons at rapidities 5.7 and 6.3.

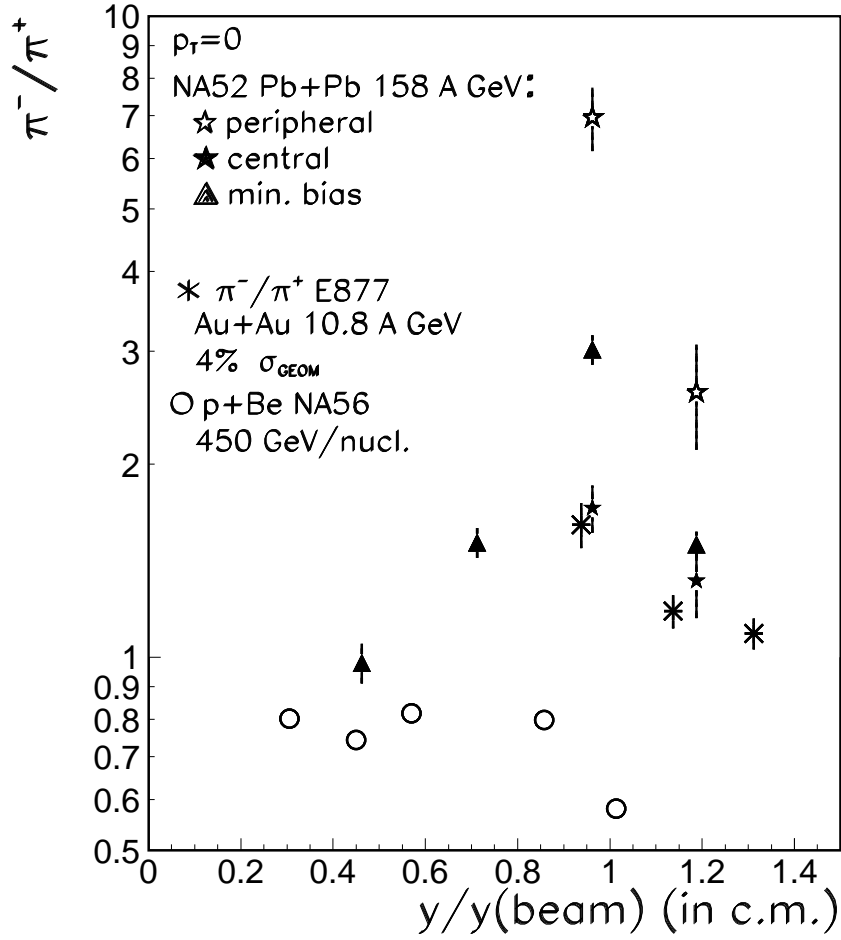


**Figure 12.**  $\pi^-/\pi^+$  ratio near zero  $p_T$  as a function of rapidity normalized to the beam rapidity in the c.m. system. NA52 data from peripheral, central and minimum bias Pb+Pb collisions at 158 A GeV are shown and compared to central Au+Au collisions at 10.8 GeV per nucleon [18] and to p+Be reactions at 450 GeV per nucleon [14].

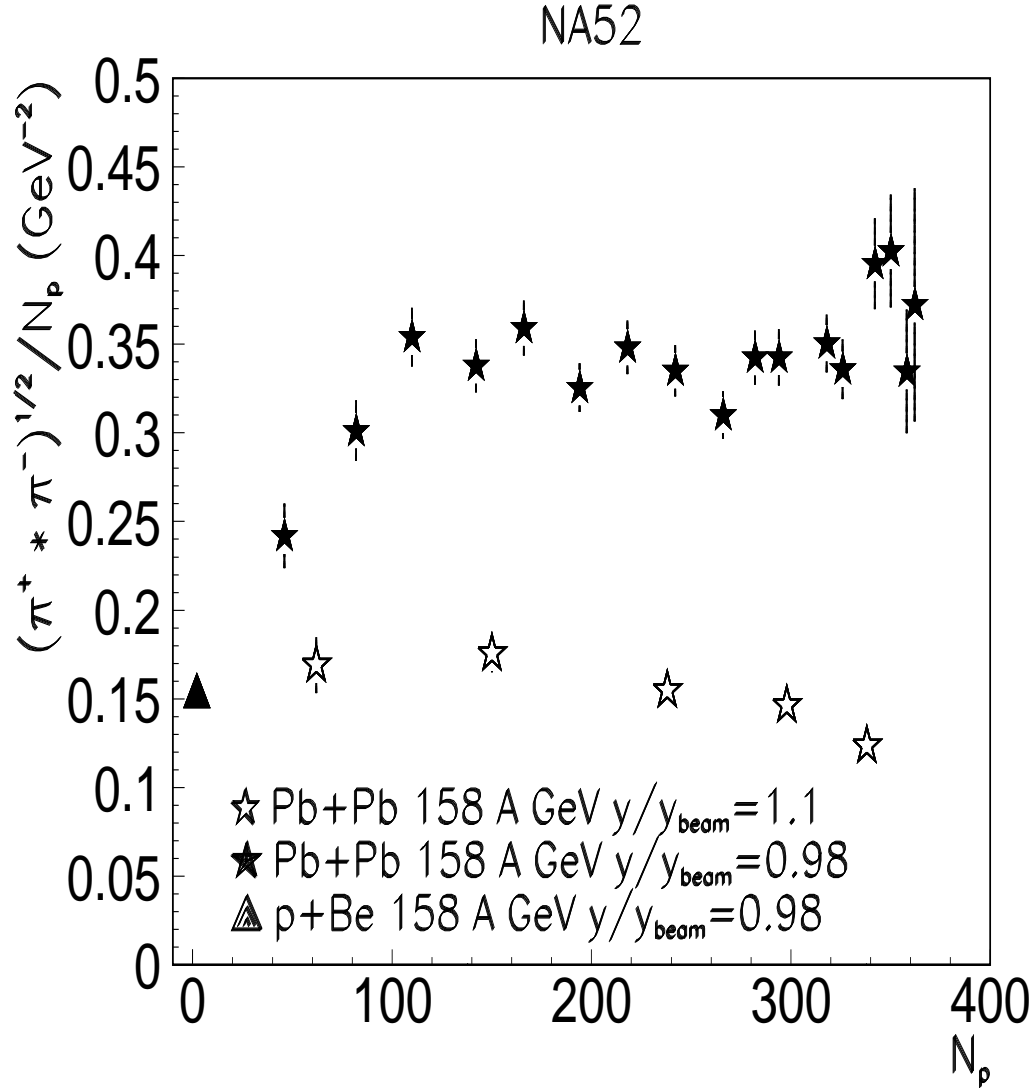


**Figure 13.** Square root of the product of the invariant differential yields ( $E d^3 N / d^3 p$ ) of the positive pions times the ones of the negative pions at  $y=5.7$  and  $6.3$  divided by the mean total number of participating nucleons  $N_p$  as a function of  $N_p$  near zero  $p_T$ . NA52 data from Pb+Pb collisions at 158 A GeV are compared to p+Be collisions measured at 450 GeV per nucleon [14], which were rescaled to 158 GeV per nucleon at similar  $p_T$  and  $y/y_{beam} \sim 0.97$  ( $y=5.7$  in Pb+Pb).

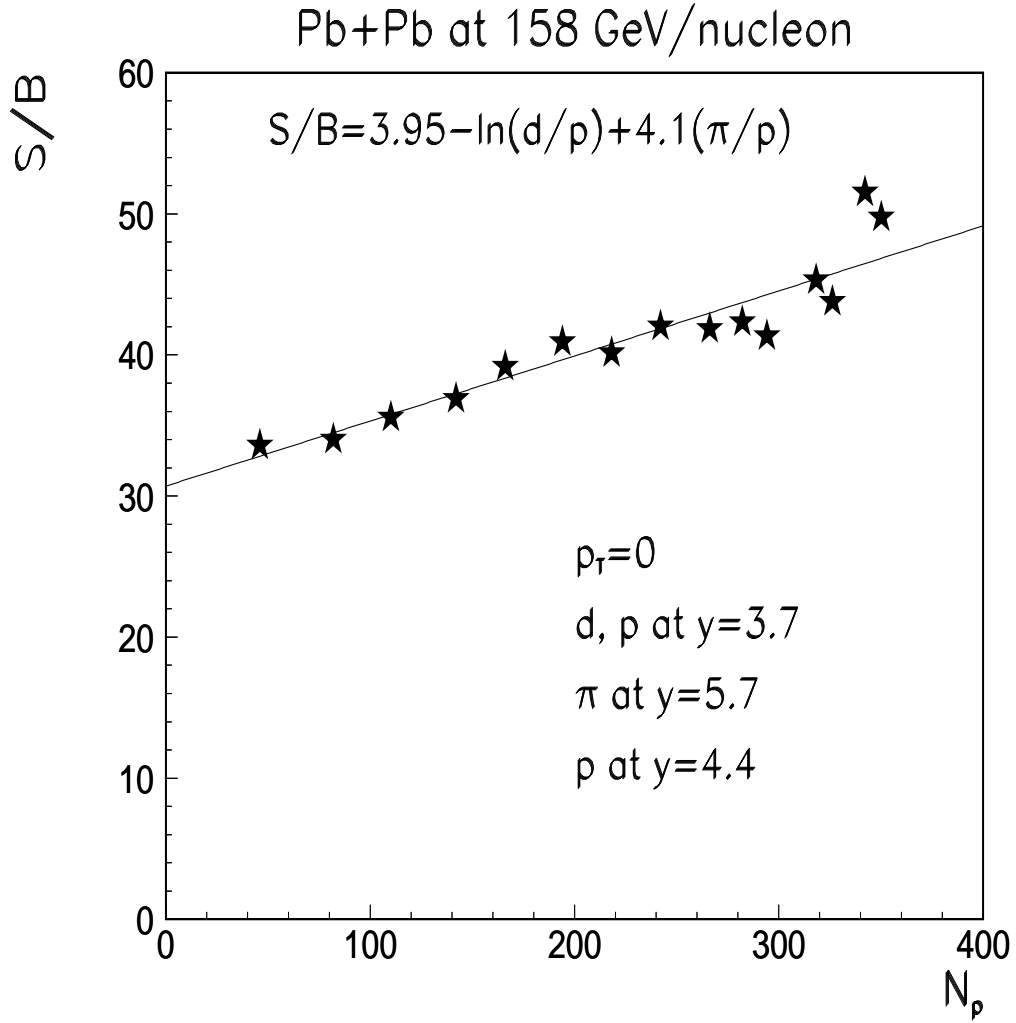


**Figure 14.** Entropy per baryon ( $S/B$ ) as a function of the number of participants in Pb+Pb collisions at 158 A GeV. (See text for explanations).